http://www.zju.edu.cn/jzus; E-mail: jzus@zju.edu.cn
ISSN 1009-3095 *Journal of Zhejiang University SCIENCE* V.5, No.1, P.86-91, Jan., 2004

Inversion of thicknesses of multi-layered structures from eddy current testing measurements

HUANG Ping-jie(黄平捷)†, WU Zhao-tong(吴昭同)

(*Institute of Advanced Manufacturing Engineering, Zhejiang University, Hangzhou 310027, China*)

†E-mail: vamadis@yahoo.com.cn

Received Mar.11, 2003; revision accepted July 3, 2003

Abstract: Luquire *et al.*'s impedance change model of a rectangular cross section probe coil above a structure with an arbitrary number of parallel layers was used to study the principle of measuring thicknesses of multi-layered structures in terms of eddy current testing voltage measurements. An experimental system for multi-layered thickness measurement was developed and several fitting models to formulate the relationships between detected impedance/voltage measurements and thickness are put forward using least square method. The determination of multi-layered thicknesses was investigated after inversing the voltage outputs of the detecting system. The best fitting and inversion models are presented.

Key words: Multi-layered structure, Thickness measurement, Eddy current testing, Multi-frequency, Inversion

Document code: A **CLC number:** TP391.7; TM13

INTRODUCTION

Thickness measurement of multi-layered structures is wildly recognized as a complex and urgent problem to tackle in many important fields. For example, the inspection of multi-layered thickness and subsurface defects (corrosion, air gap, etc.) in the lap splice of airframes and the measurement of composite deposits, etc. are of great significance to deal with in the field of non-destructive testing and evaluation (NDT&E). Due to the radiation protection problem in the radiographic inspection and the large acoustic loss in the ultrasound method, it seems these two NDE techniques are not suitable for multi-layered thickness determination with the excitation and pick-up sensor on a single side of the structure. In contrast, eddy current testing (ECT) is relatively rapid and has advantages of high sensitivity, non-contact, and low cost and can be used for thickness measurements in difficult to inspect conditions or objects such as high temperature, thin pipe, slim line and internal pore.

This paper presents the coil impedance model and the principles of eddy current testing method for determining thickness of multi-layered structures. Several regression models to fit the relationships between detected voltage and thickness are proposed and the thickness inversion algorithms are discussed. Experimental results are analyzed and the best fitting model and inversion algorithm for multi-layered thickness inspection are presented.

PROBE COIL IMPEDANCE MODEL

The numerical method used to calculate the impedance of a cylindrical, air-cored eddy-current probe coil placed over a layered conductive structure is based on the analytical solution given by Luquire *et al.* (1970) and Cheng *et al.* (1971). Fig.1 shows the geometry of the system under study, consisting of an arbitrary-layer structure where layer 1 represents the supporting structure (or air, in the absence of any support) and layer M is the outer (upper) layer of the structure. The conductivity and permeability can vary from layer to layer, but are constant in each one.

The coil impedance over the standard reference structure is (Luquire *et al.*, 1970; Cheng *et al.*, 1971):

$$Z_1 = 2K\int_0^{\infty} \frac{I^2(a)}{a^5} \cdot \Phi_1(a)\mathrm{d}a$$

The coil impedance over the structure to be detected is:

$$Z_2 = 2K\int_0^{\infty} \frac{I^2(a)}{a^5} \cdot \Phi_2(a)\mathrm{d}a$$

where $\Phi_1(a)$, $\Phi_2(a)$, are complicated functions involving the material properties of each layer (conductivity and permeability), as described in the references by Luquire *et al*. (1970), Cheng *et al*. (1971) and Huang and Wu (2002).

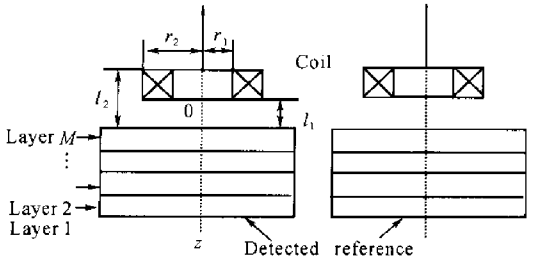

Fig.1 Coil over M layers

Left: Over detected structure; Right: Over reference structure

The impedance difference ΔZ produced by M layers on an N-turn coil is:

$$\Delta Z = Z_2 - Z_1 = K\int_0^{\infty} \frac{I^2(a)}{a^6}(\mathrm{e}^{-a\cdot l_1} - \mathrm{e}^{-a\cdot l_2})^2 \times \left(\frac{a-a_1}{a+a_1} - \frac{U_{12}}{U_{22}}\right)\mathrm{d}a \quad (1)$$

where U is the product of 2×2 matrices and can be expressed as: $U = y(a, \sigma_i, \mu_i, z_i, \omega)$, where $i = 1, 2, \cdots, M-1$; a is the separation variable; σ_i and μ_i are the permeability and conductivity, respectively, of layer i; z_i is the depth measured from the base material of the structure; ω the angular frequency;

$$K = \pi N^2 j\omega\mu_0/[(l_2 - l_1)^2(r_2 - r_1)^2];$$

$$I(a) = \int_{a\cdot r_1}^{a\cdot r_2} xJ_1(x)\mathrm{d}x.$$

According to Eq. (2), the impedance change of the coil above a layered conductive structure is a function of the parameters of the structure and the coil itself:

$$\Delta Z = F_0(r_1, r_2, l_1, l_2, \sigma_1, \sigma_2, \cdots, \sigma_M, \mu_1, \mu_2, \cdots, \mu_M, z_1, z_2, \cdots, z_{M-1}, f) \quad (2)$$

where r_1 is the inner radius of the coil, r_2 its outer radius, N the number of turns, l_1 the lift-off, l_2 the distance from upper surface of the coil to the surface of the structure. Also, μ_1 is the free space permeability, j the imaginary unit. $J_1(x)$ is the first-order Bessel function of the first kind. The interface between layers i and $i+1$ lies at a depth z_i measured from the base material of the structure; base material is layer number 1. f is the frequency of the coil.

MULTI-LAYERED THICKNESSES MEASUREMENT

According to the mathematical model [Eq. (1), Eq. (2)], the coil's impedance depends sensitively on many parameters of the structure and the coil. If the impedance change due to the variation of thickness of the structure is detected and the impedance change due to other factors is suppressed, the thickness measurement by the EC method is realized.

During the thickness estimation procedure the geometric characteristics of the coil and the properties of the structure are assumed to be known and the unknown parameter is the thickness th_i of the i-th layer. At an excitation frequency f, Eq. (2) becomes:

$$\Delta Z = F_0(z_i, f) \quad (3)$$

where,

$z_i = -(th_{M-1} + th_{M-2} + \cdots + th_{i+1} + th_i)$, at the surface of the structure, $z_i = 0$.

In practical detection, Eq. (3) can be written as:

$$\Delta U = F(z_i, f) \quad (4)$$

where ΔU is the EC inspection system output voltage due to the impedance change ΔZ of the coil.

Eqs. (3) and (4) demonstrate that the impedance/voltage change due to the variation in the i-th layer's thickness is obtained when the coil is excited at a certain frequency f_i. Thus n change values are obtained at n specific frequencies and then n thicknesses of a layered structure can be evaluated.

VOLTAGE-THICKNESS FITTING MODELS

The impedance model (1) expresses the relations between the impedance/voltage change and thickness relation is a complex problem. The following linear and non-linear fitting models were chosen at different suitable exciting frequencies respectively to fit the relations of the detected voltage ΔU_i and the known thicknesses (th_1, th_2, $\cdots$, th_i, $\cdots$, th_n) based on the least squares procedure:

1. The first-order polynomial model

$$\Delta U_i = \beta_{i0} + \beta_{i1} th_1 + \beta_{i2} th_2 + \cdots + \beta_{in} th_n + \varepsilon_i,\ i = 1, 2, \cdots, n \quad (5)$$

2. The second-order polynomial model

$$\Delta U_i = \beta_{i0} + \beta_{i1} th_1 + \beta_{i2} th_2 + \cdots + \beta_{in} th_n + \beta_{i(n+1)} th_1^2 + \beta_{i(n+2)} th_2^2 + \cdots + \beta_{i(n+n)} \cdot th_n^2 + \beta_{i(2n+1)} th_1 th_2 + \beta_{i(2n+2)} th_1 th_3 + \cdots + \beta_{i(2n+n-1)} th_1 th_n + \cdots + \varepsilon_i,\ i = 1, 2, \cdots, n \quad (6)$$

3. The third-order polynomial model

$$\Delta U_i = \beta_{i0} + \beta_{i1} th_1 + \beta_{i2} th_2 + \cdots + \beta_{in} th_n + \beta_{i(n+1)} th_1^2 + \beta_{i(n+2)} th_2^2 + \cdots + \beta_{i(n+n)} \cdot th_n^2 + \beta_{i(2n+1)} th_1^3 + \beta_{i(2n+2)} th_2^3 + \cdots + \beta_{i(2n+n)} th_n^3 + \beta_{i(3n+1)} th_1 th_2^2 + \cdots + \beta_{i(3n+n-1)} th_1 th_n^2 + \beta_{i(4n)} th_1^2 th_2 + \cdots + \beta_{i(4n+n-1)} th_1^2 th_n + \beta_{i(5n)} th_1 th_2 + \beta_{i(5n+1)} \cdot th_1 th_3 + \cdots + \beta_{i(5n+n-2)} th_1 th_n + \beta_{i(6n-1)} \cdot th_2 th_3 + \cdots + \varepsilon_i,\ i = 1, 2, \cdots, n \quad (7)$$

4. The third-order + log polynomial model

$$\Delta U_i = \beta_{i0} + \beta_{i1} \log(th_1) + \beta_{i2} th_2 + \cdots + \beta_{in} th_n + \beta_{i(n+1)} (\log(th_1))^2 + \beta_{i(n+2)} th_2^2 + \cdots + \beta_{i(n+n)} th_n^2 + \beta_{i(2n+1)} (\log(th_1))^3 + \beta_{i(2n+2)} th_2^3 + \cdots + \beta_{i(2n+n)} th_n^3 + \beta_{i(3n+1)} \log(th_1) th_2^2 + \cdots + \beta_{i(3n+n-1)} \cdot \log(th_1) th_n^2 + \beta_{i(4n)} (\log(th_1))^2 th_2 + \cdots + \beta_{i(4n+n-1)} (\log(th_1))^2 th_n + \beta_{i(5n)} \log(th_1) \cdot th_2 + \beta_{i(5n+1)} \log(th_1) th_3 + \cdots + \beta_{i(5n+n-2)} \cdot \log(th_1) th_n + \beta_{i(6n-1)} th_2 th_3 + \cdots + \varepsilon_i,\ i = 1, 2, \cdots, n \quad (8)$$

5. The exponential function model

$$\Delta U_i = e^{\beta_0 + \beta_{i1} th_1 + \beta_{i2} th_2 + \cdots + \beta_{in} th_n} \varepsilon_i,\ i = 1, 2, \cdots, n \quad (9)$$

6. The power + exponential function model

$$\Delta U_i = \beta_{i0} th_1^{\beta_{i1}} e^{\beta_{i2} th_2} th_3^{\beta_{i3}} e^{\beta_{i4} th_4} \times \cdots \times th_{n-1}^{\beta_{i(n-1)}} e^{\beta_{in} th_n} \varepsilon_i,\ i = 1, 2, \cdots, n \quad (10)$$

where n – the sum of the layers to be tested; β_i – fitted model parameters; ε_i – random variation. Two layers of a 4-layer structure were tested, so $n = 2$.

INVERSION ALGORITHM

Analysis showed that at n exciting frequencies n thicknesses can be detected. The magnetic flux of the coil should penetrate into the substrate of the structure. At frequency f_i, the detected voltage changes vary when the combination of thicknesses of each layer varies. Use of the above fitting models yielded the relations between voltage and thickness and the coefficients of various formulas [Eq.(5) – Eq.(10)]. The goodness of fitting of each equation is evaluated and then the best fitting model is selected. The fitting results at different exciting frequencies (f_1, f_2, $\cdots$, f_n) are as follows:

$$\Delta U_i = F_i(th_1, th_2, \cdots, th_n),\ i = 1, 2, \cdots, n \quad (11)$$

Eq.(11) is linear independent and then a numerical optimization can be applied to solve/inverse the thicknesses (th_1, th_2, $\cdots$, th_n):

$$\min_{\substack{th_i \geqslant 0, \\ i = 1, 2, \cdots, n}} \sum_{i=1}^{n} \sum_{j=1}^{m} \left| f_{ij}(th_1, th_2, \cdots, th_i, \cdots, th_n) - \Delta U_{ij} \right|^2 = \min F(th_i) \quad (12)$$

where $i = 1, 2, \cdots, n$ – the sum of layers to be tested; $j = 1, 2, \cdots, m$ – the number of experimental data set at each frequency; ΔU_{ij} – detected voltage of the j-th combination of thicknesses at f_i.

Eq.(12) presents an unconstrained optimization problem so the Quasi-Newton method can be adopted to solve it. The computing steps are shown in Fig.2.

Thus the relationships between thicknesses th_1, th_2, $\cdots$, th_n and the output voltage ΔU_1, ΔU_2, $\cdots$, ΔU_n are obtained as

$$th_i = g_i(\Delta U_1, \Delta U_2, \cdots, \Delta U_n),\ i = 1, 2, \cdots, n \quad (13)$$

Eq.(13) shows that during measurement of n – layer thicknesses each thickness th_i can be described as a function containing n variables – voltage changes($\Delta U_1, \Delta U_2, \cdots, \Delta U_n$) at different frequencies. If $n = 1$ the problem becomes single layer thickness determination. The Quasi-Newton method has second-order convergence property and the starting point of iterations should be selected based on prior knowledge or the known conditions.

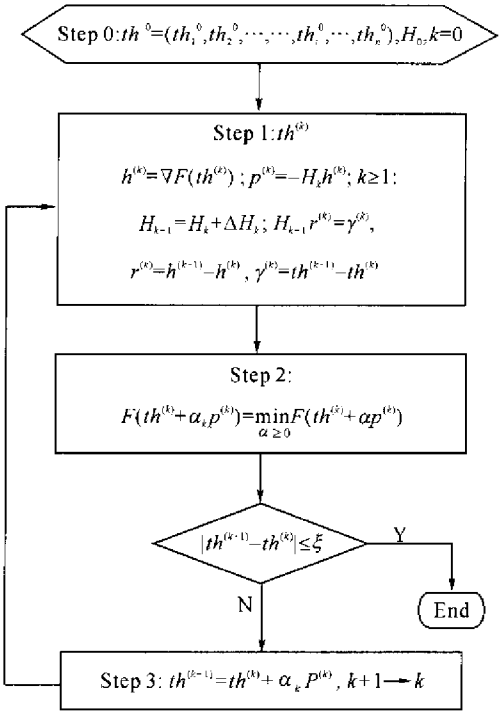

Fig. 2 The flowchart of the Quasi-Newton method H, the Hessian matrix; ξ, tolerance; $p^{(k)}$, search direction; α_k, iterating step length

EXPERIMENTS AND RESULTS

Experimental system and detected objects

The schematic diagram of the eddy current testing instrument is shown in Fig. 3. Two probes working in differential mode can reduce the environmental interference are used in the instrument. Operation frequency is selected by the frequency switch.

The application studied is the case of the coils over a multi-layered structure which is a special case for $M = 4$, as shown in Fig. 1. It is used to simulate the double layer skin of an airframe or the similar structures found in the stamping process where the outer layer thickness and the inner corrosion or air-gap size are to be determined. The known parameters are: coil parameters: $N = 330$, $r_1 = 3.0$ mm, $r_2 = 5.11$ mm, $l_2 - l_1 = 20.70$ mm, $L_1 = 1.02$ mH, $R_1 = 19.84\ \Omega$; $l_1 = 0.0$ mm; layer 1 – air: $\sigma_1 = 0$, $\mu_1 = \mu_0$, $th_1 = 0$; layer 2 – aluminum alloy: $\sigma_2 = 18.5$ MS/m, $\mu_2 = \mu_0$, $th_2 = 4.0$ mm; layer 3 – air: $\sigma_3 = 0$, $\mu_3 = \mu_0$; layer 4 – aluminum alloy: $\sigma_4 = 18.5$ MS/m, $\mu_4 = \mu_0$(Fig. 1).

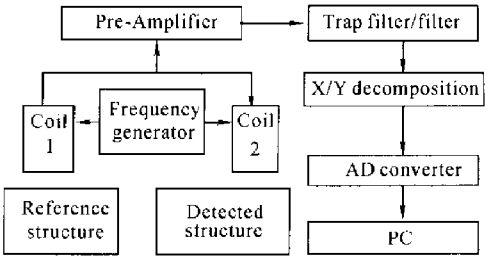

Fig. 3 Schematic representation of the inspection system

Three different data sets at three different excitation frequencies: f_1, f_2 and f_3 were measured and three fitting processes were carried out. The obtained voltage change – thickness expressions [$\Delta U_i = F_i(th_4, th_3)$] were substituted into the approximating model Eq.(12) pairwise and thus th_4, th_3 were inversed from the voltage measurements.

Selection of frequency

For eddy current measurement of multi-layered structure thicknesses, the frequency should be chosen to maximize the change in impedance to a change in thicknesses for a given coil. References (Rekanos *et al.*, 1997; American Society for NDT, 1998) gave an expression that can be used with nonmagnetic materials for this problem: $\delta = 1/\sqrt{\pi f \mu \sigma}$, where δ is the standard penetration depth of eddy current and is recommended to be 1.2 times as deep as the thickness of the structure. The result shows that the excitation frequency can be calculated by $f = 1.6\rho/th^2$, where $\rho = 1/\sigma$($\mu\ \Omega$ cm), here f's unit is kHz, μ is the permeability of nonmagnetic materials, th is thickness(mm).

For this application the range of optimum frequencies can be calculated as: $f = 0.096 - 0.95$ kHz. In our experiments, the following 3 frequencies were chosen: $f_1 = 200$ Hz, $f_2 = 400$ Hz, $f_3 = 800$ Hz.

Fittng models analysis

Experiments carried out at 3 different frequencies showed that the sum of datasets could be divided into 66 groups. Data were fitted using the fitting models [Eqs.(5) – (10)] introduced and the coefficients of fitting models were calculated as given in Table 1.

Table 1 Fitting results of voltage-thickness relation

RSS	200 Hz	400 Hz	800 Hz
1st-order	0.054580	0.490198	0.007608
2nd-order	0.00885	0.045591	0.001490
3rd-order	0.002501	0.012951	0.000324
3rd-order + log	0.001282	0.012994	0.000180
Exponential	0.009216	0.311167	0.002828
Power + Exp	0.038865	0.315883	0.003091

Comparison of each model's fitting goodness using the residual sum of squares (RSS) as the criterion is shown in Table 2 (The random error ε_i of the exponential model and power + exponential model should be calculated as $\log(\varepsilon_i)$). Table 2 shows that the fitting result of the third-order polynomial model is better than the second-order one; that the linear model is worst; and that the inspection result at 200 Hz is better than 400 Hz. The RSS is smallest at 800 Hz, at which frequency the sensitivity of the system is found to be worst. The fitting curves of the third-order and linear models at 200 Hz are shown in Fig.4 and Fig.5. They also confirm the above analysis.

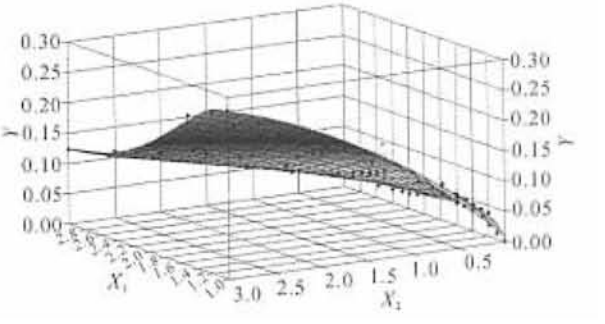

Fig.4 Fitting graph of 3rd-order model(200Hz)
Black points, measurements: X_1, th_4; X_2, th_3; Y, ΔU

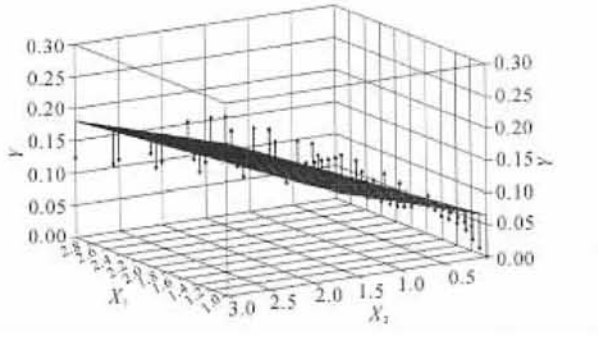

Fig.5 Fitting graph of 1st-order model(200Hz)
Black points, measurements: X_1, th_4; X_2, th_3; Y, ΔU

Table 2 Coefficients of voltage change-thickness fitting models[Eqs.(5) – (10)]

Hz		β_0	β_1	β_2	β_3	β_4	β_5	β_6	β_7	β_8	β_9
200	1st-order	0.0936	−0.0281	0.0571							
	2nd-order	0.0545	−0.0309	0.1405	0.0099	−0.0061	−0.0356				
	3rd-order	−0.2238	0.4204	0.2235	−0.2192	−0.0300	−0.0918	0.0370	0.0008	0.0109	0.0065
	3rd-order + log	0.0097	0.2051	0.14275	−0.4281	−0.0208	−0.1074	0.2590	0.0008	0.0208	−0.0127
	Exponential	−2.2486	−0.3838	0.4824							
400	1st-order	0.1808	−0.0528	0.1396							
	2nd-order	0.0829	−0.0827	0.3769	0.0365	−0.0104	−0.1117				
	3rd-order	−0.4472	0.7404	0.6006	−0.3605	−0.0488	−0.2975	0.0615	−0.0032	0.0282	0.0270
	3rd-order + log	−0.0120	0.3769	0.3410	−0.6805	−0.0252	−0.3129	0.4570	−0.0032	0.0529	−0.0360
	Exponential	−1.4640	−0.4195	0.5337							
800	1st-order	0.0282	−0.0119	0.0088							
	2nd-order	0.0493	−0.0513	0.0345	0.0129	−0.0015	−0.0113				
	3rd-order	−0.0561	0.1107	0.0762	−0.0631	−0.006	−0.052	0.0112	−0.0002	0.0029	0.0082
	3rd-order + log	0.0003	0.0699	0.0349	−0.1766	−0.0037	−0.0547	0.1115	−0.0002	0.0056	0.0159
	Exponential	−2.8322	−1.307	0.5214							

Inversion calculation analysis

The fitted voltage change vs thickness relations are substituted into inversion model Eq. (12) pairwise: 200 Hz and 400 Hz, 200 Hz and 800 Hz and 400 Hz and 800 Hz. The Quasi-Newton iteration method were used to calculate the thickness values of layer 4 and layer 3. The initial value of th_4 in the procedure of iterations should be determined in response to the known conditions and the starting value of th_3 is comparatively not strict. It was found that the combination of 200 Hz and 400 Hz had the best inversion results; and that the inversion errors for layer 4 (outer layer) were smaller than those of layer 3 (inner layer) (See Table 3).

Table 3 Inversion errors comparison
(MAE: mean absolute error; L.: Layer)

Hz	200&400		200&800		400&800	
	L.4	L.3	L.4	L.3	L.4	L.3
MAE (mm)	1.12 E-4	3.82 E-4	8.79 E-4	2.50 E-4	9.02 E-4	5.63 E-4

Inversion results are shown partly in Table 4. They are the data at 200 Hz and 400 Hz and the fitting model is 'third-order polynomial + log'. It is obvious that the inversion error increases when the thickness of layer 4 increases and the inversion error decreases when the thickness of layer 3 increases. The explanation is that during the thickness inspection of lap splices, detection accuracy decreases as the outer thickness increases. Difficulty of inspection increases as the size of the inner corrosion or air gap decreases. But, generally speaking, the inspection results are promising.

Table 4 Thickness inversion results
(L.: Layer; *Th*: Thickness; *Inv*: Inversion; *Er*: Error)

L.4			L.3		
Th (mm)	*Inv* (mm)	*InvEr* (%)	*Th* (mm)	*Inv* (mm)	*InvEr* (%)
1	1.007	0.74	0	0.010	/
1	0.996	0.37	0.08	0.178	2
1	1.022	2.22	0.5	0.525	5.04
1	1.012	1.16	1	1.028	2.78
1	0.998	0.21	1.5	1.476	1.573
1.2	1.200	0.025	0	0.001	/
1.2	1.195	0.383	0.34	0.315	7.412
1.2	1.204	0.317	0.5	0.543	8.58
1.2	1.191	0.692	1	1.022	2.15
1.2	1.205	0.425	1.5	1.491	0.627
1.5	1.490	0.667	0	−0.066	/
1.5	1.502	0.16	0.34	0.316	7.206
1.5	1.499	0.02	0.5	0.501	0.12
1.5	1.473	1.78	1	1.031	3.13
1.5	1.451	3.293	1.5	1.538	2.5

CONCLUSIONS

The mathematical impedance model was used to study the principles of thickness measurements of multi-layered structure. Several fitting models for mapping the relationships between detected voltage change and thickness are proposed and the approximate model to inverse thicknesses is presented. The determination of thicknesses of a 4-layer structure is studied and an inspection system is developed. The experimental results showed that the techniques and algorithms studied are reasonable and feasible. Our further work is to optimize coil geometry parameters and the excitation current frequency in terms of the simulation programs and to carry out this research in more applications.

References

American Society for Nondestructive Testing, 1998. Nondestructive Testing Handbook, Electromagnetic, Edition 4.

Cheng, C.C., Dodd, C.V. and Deeds, W.E., 1971. General analysis of probe coils near stratified conductors. *Int. J. Nondestr. Test*, **3**: 109 – 130.

Huang, P.J. and Wu, Z.T., 2002. Thickness measurement of multi-layered structure by eddy current testing. *Proceedings of ISIST'2002*, The Press in Harbin Insititute of Technology, Harbin, **5**: 38 – 42.

Luquire, J.W., Deeds, W.E. and Dodd, C.V., 1970. Alternating current distribution between planar conductors. *Journal of Applied Physics*, **41**(10): 3983 – 3991.

Oystein, B., 1993. Model-based inversion of plate thickness and liftoff from eddy current probe coil measurements. *Materials Evaluation*, **Jan**: 72 – 76.

Rekanos, I.T., Theodoulidis, T.P., Panas, S.M., Tsiboukis, T.D., 1997. Impedance inversion in eddy current testing of layered planar structures via neural networks. *NDT&E International*, **30**(2): 69 – 74.

Wu, Z.T., and Huang, P.J., 2002. Impedance Model Simulation and Verification of Thickness Multi-layered Structure Measurement using Eddy Current Method. Proceedings of the 4th Symposium on Metrological Science and Technology, Taiwan, **c11**: 1 – 7.

Yan, R.C., 1996. Thickness measurement using eddy current method. *Nondestructive Testing*, **18**(6): 169 – 172.